Published online in 2010 as part of U.S. Geological Survey Scientific Investigations Report 2010-5091.

A Particle Tracking Technique for Bedload Motion

Athanasios (Thanos) N. Papanicolaou[1] and Doug Knapp[2]

[1]Associate Professor, Robert and Virginia Wheeler Faculty Fellow in Engineering, IIHR-Hydroscience and Engineering, The University of Iowa, Iowa City, Iowa, United States, [2]Seattle District Army Corps of Engineers, Seattle, Washington, United States.

ABSTRACT

The objective of this research was two-fold. First, it was designed to test the ability of the Gravel Transport Sensor (GTS) to accurately detect moving particles in a streambed under a variety of flow conditions. The second objective was to develop an equation that provides the velocity of individual particles and use this equation to estimate the flux of sediment particles impinging the GTS. Tests were preformed in a 0.5 m wide and 15 m long water-recirculating flume. The prototype GTS cylinder was 59 and 567 mm in diameter and length, respectfully. The tests used uniform spherical glass particles, which eliminated any variance that might arise due to the shape of the particles or composition of the bed and allowed the study to focus on the ability of the GTS to detect particles. An artificial bed of well-packed 8 mm glass beads was used to provide a uniform roughness and eliminate hiding and embeddedness effects over the test section. These particles where glued in place around the cylinder to prevent scour. Three particle sizes, 25.4, 22.2, and 15.9 mm in diameter (1, 7/8, and 5/8 in), were tested over six different flow conditions. All tests were conducted under uniform flow conditions. The GTS recorded 20 samples per output with an interval of 5 seconds. Data for bedload rate, velocity profile, flow depth, flow rate, recorded impacts by GTS, and actual impacts on GTS where collected for each test. While, the second objective of the study was met and a relation between the flow and particle velocities was developed, the performance of the prototype GTS used in this study was considered unsatisfactory. Recommendations are made to alter the geometric shape of the GTS to prevent flow reversal at the frontal face of the instrument and thus increase the number of particles hitting the cylinder.

1. INTRODUCTION

Several methods are commonly used to measure sediment transport, including detention ponds, various observation methods, and the use of both portable and stationary samplers.

The most common means of sampling bedload is by portable samplers. Bedload discharge estimates are made from portable samplers, such as the Helley-Smith sampler (Figure 1a). The sampler is placed on the bed of the channel and sediment is collected and analyzed.

Stationary samplers are samplers designed to be placed and left in place for operation. They come in several forms. A detention pond can be utilized for capturing sediment for measurement by diverting a stream through a pond (Figure 1b). All material moved as either bedload or in suspension is effectively trapped by the stilling effects of the pond (Leaf, 1970; Troendle, et al., 1996). Each fall, after

runoff from snowmelt recedes, the ponds are drained and the accumulated sediment is excavated. The total sediment volume is calculated using surveyed data of the difference in bed elevation (Ryan and Troendle, 1997). This method yields an annual transport and can be correlated with flow conditions for that year. Similarly, the recording bedload trap sampler is another example of a stationary sampler where bedload falls or rolls into a trap that extends across the bottom of the channel (Figure 1c).

Bedload measurements can also be made by observation of tracer particles before and after a flow event. There are two basic methods of observation. The first is known as ”seeding,” where individual particles are gathered, painted, and replaced with their positions marked during low flow. After a flow event, any movement of the particles from their original marked location is considered particle transport (Ryan and Troendle, 1997). The second is the “painted area” method. An exposed portion of the bed is painted and photographed while the stream is at a low stage. After a flow event, the painted area is again photographed. Non-colored particles inside the painted region are considered to be transported bedload (Ryan and Troendle, 1997).

Another development is the magnetic tracer technique, which makes use of the naturally magnetic pebbles and cobbles of the riverbed. When a magnetic pebble crosses the detector log, a voltage peak is induced according to the Faraday inductive principle (Bunte, 1992). The sediment is then collected in sampling net behind the sensor.

Recently, other tracer particles have been used as predictors of bedload transport. Specifically, “spy cobbles” have been developed that are equipped with a geographic positioning system (GPS) to track the pathway of bedload particles in natural streams and their traveling (displacement) distances (Figure 1d). Also, in the laboratory, advancements in video imaging have eased the process of tracking particle displacement to determine the displacement velocity of particles and relate it to bedload (Papanicolaou et al., 1999).

***Limitations of existing devices*:** Each of these methods of measurement has some limitations in terms of providing local measurements or a continuous bedload transport estimate. Local measurements of bedload can be of high importance around hydraulic structures (e.g., barbs, bridge piers). Existing methods such as detention ponds were inherently designed to yield an annual flux of sediment and are, therefore, unable to provide bedload rates during a single flow event, with the latter being data that are currently missing in the literature (Ryan and Troendle, 1997).

The seeded particles technique is a technique that has been often used for making local bedload observations but not on a continuous basis since this method requires significant manual involvement. Particles are usually placed atop the gravel bed. However, when particles are removed and replaced, as in the case of seeded particles, the particles become more susceptible to movement. Bed material tends to orient itself into the most stable form possible. This will most likely cause the seeded particles to move to a more stable position and can lead to an overestimation of bedload rate. Particle sizes may also be distorted by overlaying particles or by the orientation of the picture plane (Church et al., 1987).

Similarly, portable samplers show low efficiency in trapping large sized particles. The size of the particles that can be sampled is limited by the opening of the sampler. The magnetic tracer technique employed by Bunte (1992) is a good improvement on being able to capture the largest size fractions and being less intrusive, but it is not without. The sample only covers portions of the active channel and takes at least three people to collect (Bunte, 1992). This means that a good understanding of where the bedload is occurring in the channel is vital in correctly placing the device the first time. The tracer is also constricted to a short sampling duration and is unable to capture particles less than 10mm (Bunte, 1992).

Most of these techniques lack the ability to make local measurements, i.e. transport induced from a pier, fish passage culverts, large particle, or bedform. Portable samplers such as a Helley-Smith are non-applicable to steep mountain streams where the bed is dominated by non-uniform gravel. The development of an accurate, portable, non-intrusive instrument is vital in order to have a better

understanding of the hydraulic, morphologic, and sedimentation processes in gravel rivers for preservation and restoration of these natural resources.

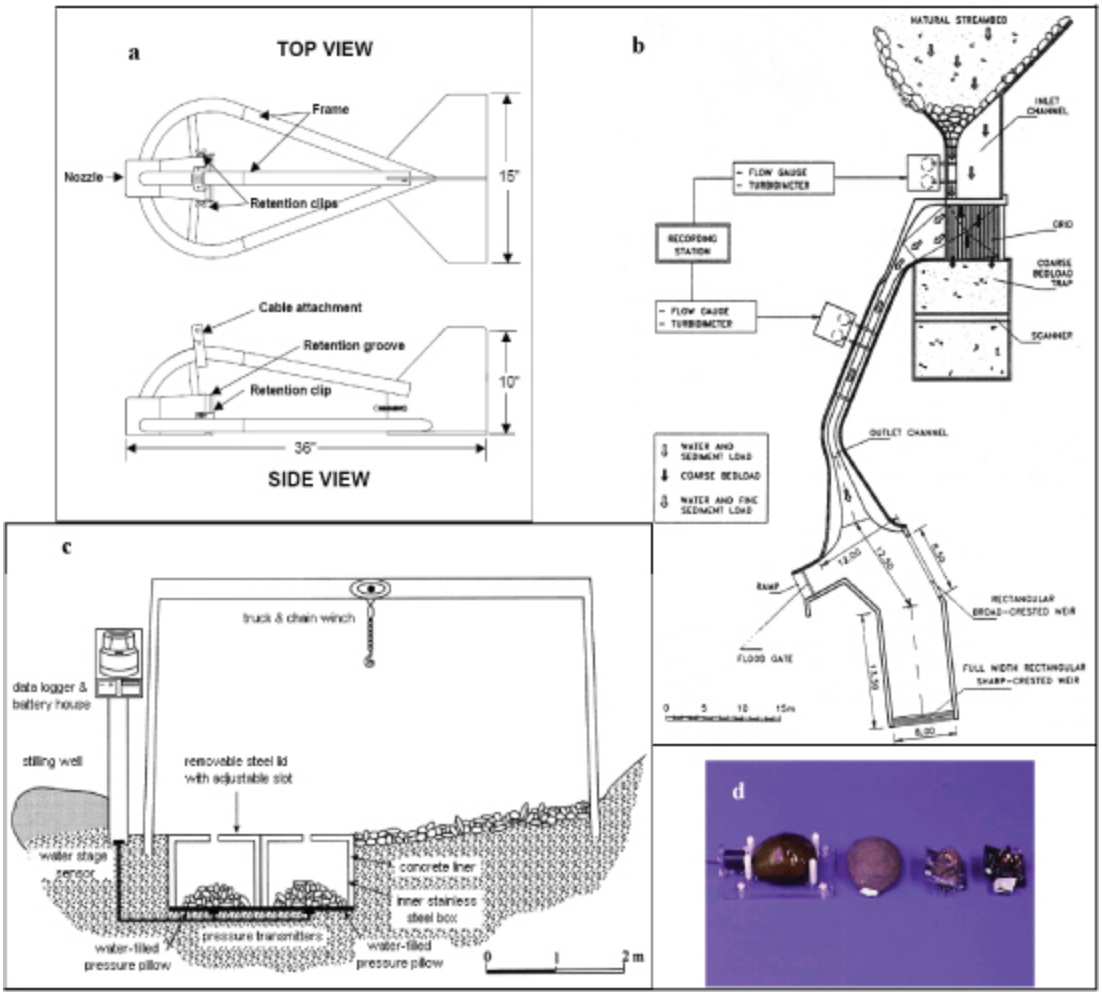

Figure 1. Sediment sampling instruments: a) Helley-Smith bedload sampler; b) plan view of diversion bedload sampling station; c) section of a recording bedload sampler; d) tracer particles "Spy Cobbles".

2. GRAVEL TRANSPORT SENSOR (GTS)

The Gravel Transport Sensor (GTS) (Figure 2) was developed by John Downing of D & A Instruments in Port Townsend, WA, which was recently bought by Cambell International. It is an acoustic device that detects moving sediment particles as they impact a steel pipe, accumulates a count of impacts, and stores a record of the impacts at a regular interval.

Published online in 2010 as part of U.S. Geological Survey Scientific Investigations Report 2010-5091.

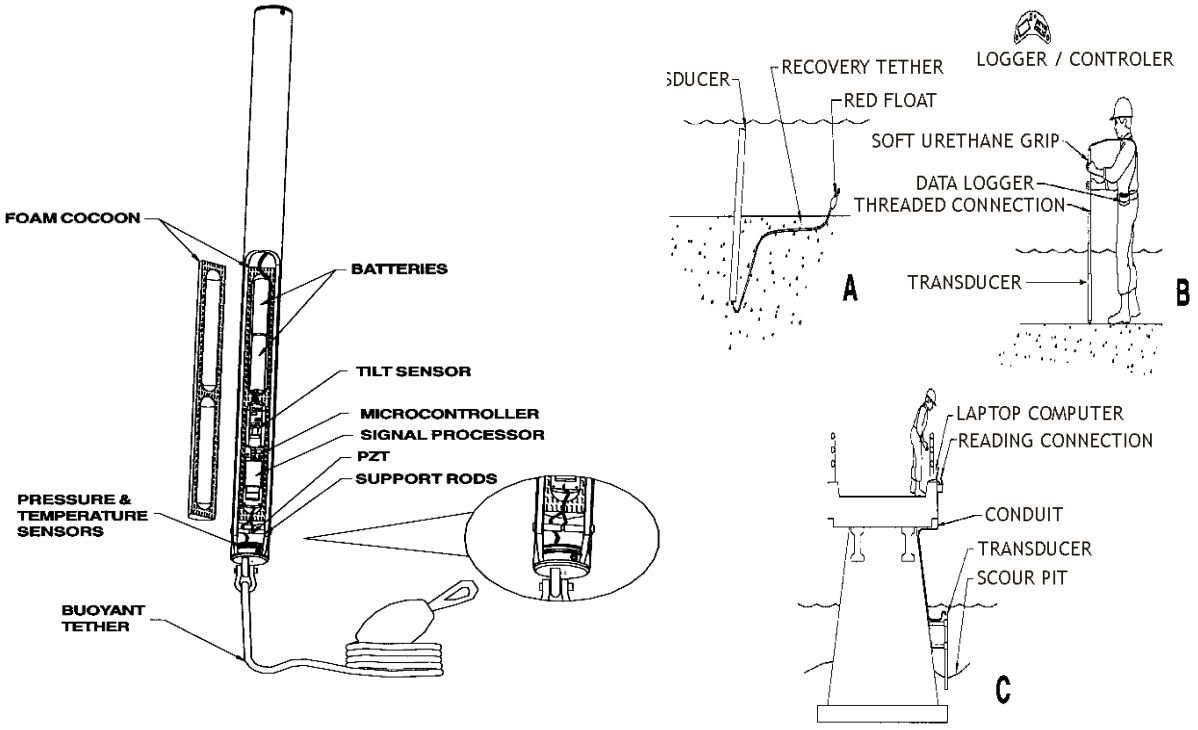

Figure 2. A sketch of the GTS system and its different uses (after Downing, 1999).

The GTS is able to detect particles ranging from 10 mm to 128 mm in size moving as bedload, i.e., rolling, sliding, or bouncing (Downing, 1999). The GTS has the potential to become a useful tool in measuring bedload in gravel bed streams and rivers, gravel beaches, and gravel talus slopes (Downing, 1999). The GTS can have sampling periods and duration times downloaded to it from a computer and then be placed in the active layer or attached to a pier and left for up to 5 months at a time. The recorded information can then be downloaded to the computer for data analysis.

In operation, moving particles strike the GTS cylinder and excite damped vibrations in the cylinder that are picked up by a piezoelectric vibration sensor (PZT). The electrical signal produced by the PZT is detected, amplified, and produces a signal. The first part of the signal is a high frequency, rapidly decaying ping that is followed by resonant ringing of the cylinder (Downing, 1999). In order to avoid masking a new impact, an 8^{th} order high pass filter is used to remove the ringing. An analog circuit processes the signals, rejects flow and bedload noise, and uses an adaptive filter to a comparator to output logic pulses for counting (Downing, 1999).

3. OBJECTIVE

The objective of this research was two-fold. First, it was designed to test the ability of the GTS to accurately detect moving particles in a streambed under a variety of flow conditions. The second objective was to develop an equation that provides the velocity of individual particles and use this equation to estimate the flux of sediment particles impinging the GTS.

3.1 Testing of the GTS

Tests were preformed in a 0.5 m wide and 15 m long water-recirculating flume. The prototype GTS cylinder was 59 and 567 mm in diameter and length respectfully. All tests used uniform spherical glass particles, which eliminated any variance that might arise due to the shape of the particles or composition of the bed and allowed the study to focus on the ability of the GTS to detect particles. An artificial bed of well-packed 8 mm glass beads was used to provide a uniform roughness and eliminate hiding and embeddedness effects over the test section. These particles where glued in place around the cylinder to prevent scour. Three particle sizes, 25.4, 22.2, and 15.9 mm in diameter (1, 7/8, and 5/8 in), were tested over six different flow conditions. Particles were placed at a distance of 4.5 to 6 particle diameters apart. This was to prevent "grouping" of particles during the tests, even though this may not represent the bed conditions in the stream at all times. Figure 3 shows a setup of the test section. Velocity measurements were made along the vertical axis with a Swoffer 2100 current meter, and flow rates were measured with a sharp crested weir. A video camera was mounted above the GTS to monitor particle behavior around the cylinder.

All tests were conducted under uniform flow conditions. The GTS recorded 20 samples per output with an interval of 5 seconds. Data for bedload rate, velocity profile, flow depth, flow rate, recorded impacts by GTS, and actual impacts on GTS where collected for each test.

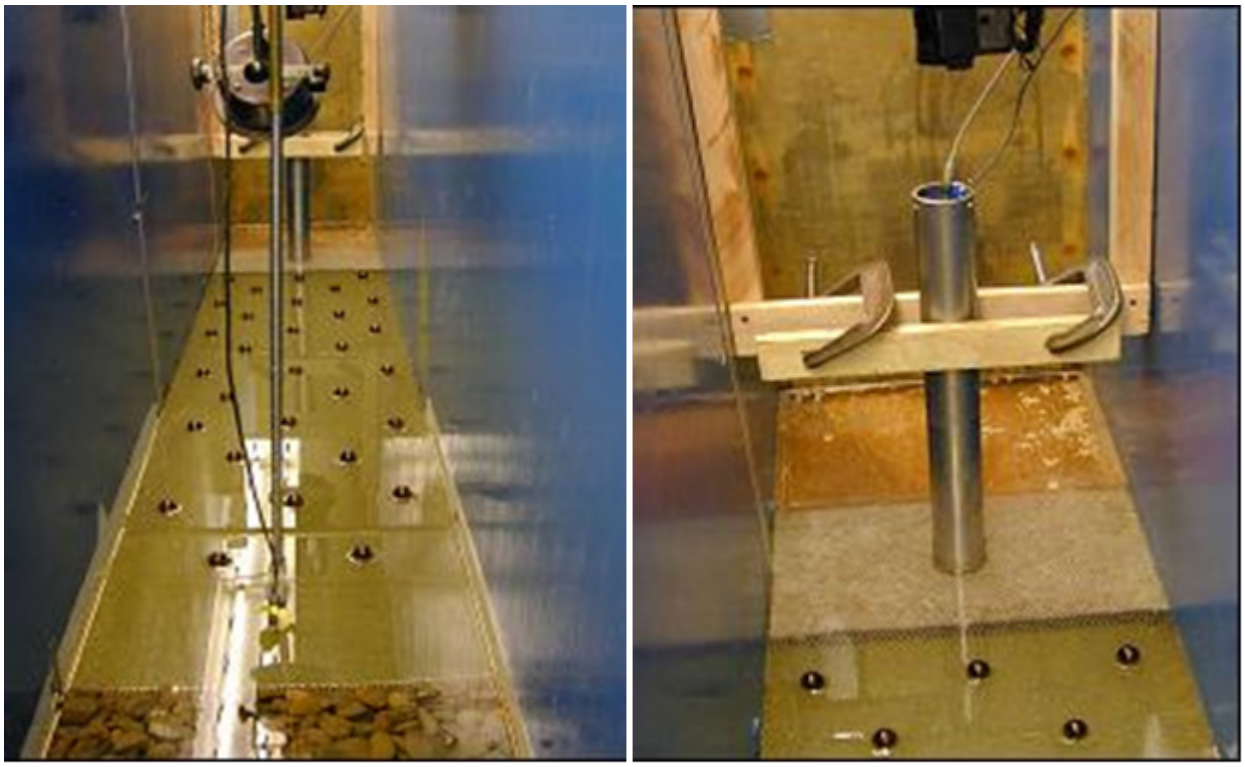

Figure 3. Test section and GTS setup.

Preliminary analysis of uniformly sized sediment experiments has clearly shown that a linear correlation exists between the ping rate (expressed in Hz) and sediment flux (expressed in Kg/m/s) (Figure 4). These tests were conducted six times, each time using different size spheres, and they are only applicable to uniform sized gravel. In the present study, this limitation was removed by performing

experiments with different-sized gravel. The major thrust of this project was the development of a method that converts sediment momentum measurements to sediment flux measurements when sediment particles of different sizes are transported and hitting the GTS. Once the correlation between the pings rates and the momentum of the particles colliding with the GTS is determined, we will utilize the momentum equation along with the fluid velocity (assuming a zero time lag between fluid and particle motion) in order to determine the masses of the particles.

To convert momentum to sediment flux, the theory of fractional sediment transport was considered. According to this theory, if there are i-different gravel sizes present atop a stream bed with diameter di, (i in this study varies between 1-3 since three particle sizes, 25.4, 22.2, and 15.9 mm have been considered) then F_i denotes the fraction of sediment found atop the stream having diameter d_i, m_i is the mass of an individual grain with size d_i, and Y_i is a mobility coefficient. If $Yi = 1$ it implies that all particles with an average diameter d_i have the same response and mobility to changing flow conditions. The total mass of sediment with size d_i will be equal to,

$$M_i = \sum \left(m_i \frac{F_i}{d^2 i} Y_i \right) \tag{1}$$

and the momentum J_i of each i-fraction will be,

$$J_i = \sum M_i U_{Pi} \tag{2}$$

Where, Up_i is the particle velocity with size i. The momentum J_i is provided by the GTS while the particle velocity is determined via a dimensional analysis and the complementary use of data.

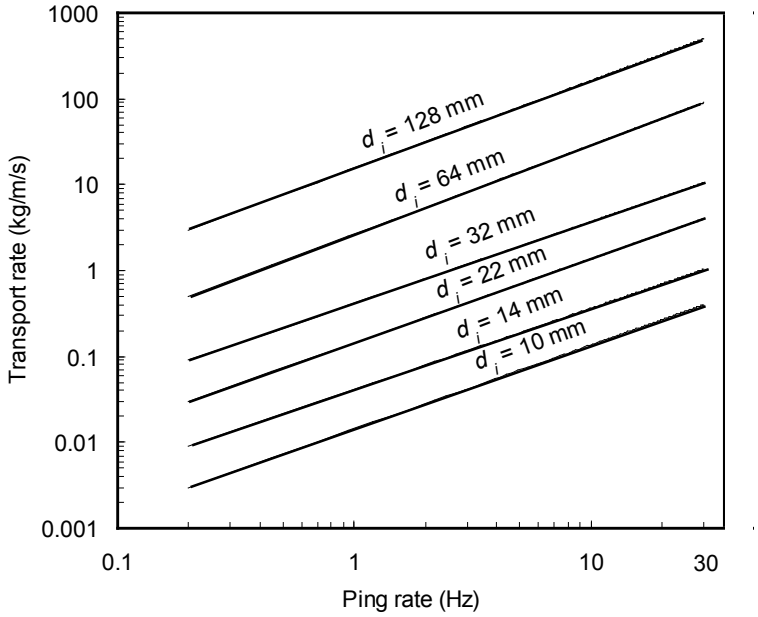

Figure 4. Sediment flux versus "ping" rate (after Downing, 1999).

3.2 Determination of the Particle Velocity

The majority of the particle monitoring was performed in the same flume (15 m long and 0.5 m wide) with a stationary slope of zero. Complementary runs were also conducted in a larger tilting flume that is 21 m long and 0.91 m wide. The rolling motion of four groups of spherical particles with

diameters of 8mm, 15.9 mm, 22.2 mm, and 25.4 mm was monitored for varying flow conditions and bed roughness. The flow conditions ranged from the incipient condition to flows causing general sediment motion. Bed roughness conditions were simulated by using spheres with diameters of 8 mm and 19 mm and a gravel bed with a median sediment size of 6.5 mm. The thickness of the simulated roughness bed was about 3.5 cm. The bed was flattened to avoid protrusion effects and was well compacted to allow the unimpeded transport of the entrainable spheres.

An Acoustic Doppler Velocimeter (ADV) and a Swoffer 2100 current meter were used to obtain the velocity profiles throughout the water depth and flow rates were measured with a sharp crested weir. The velocity profiles were used in conjunction with the Clauser method to determine the friction velocity. The Clauser method was necessary since the shear velocity expression

$$U_* = \sqrt{gRS} \tag{3}$$

where g is the gravitational acceleration, R is the hydraulic radius and S is the bed slope, cannot be used with a slope of zero that was present in some of the bed conditions. Incipient flow conditions were determined based on a trial and error method and were defined as the conditions corresponding to the dislodgment of individual particles from their initial position (Papanicolaou et al., 2002).

A digital camera captured the particle movement over a flat bed. The camera was mounted above the flume in order to obtain a plan view of the bed. Individual pictures depicting particle motion were obtained using Asymetrix DVP and Adobe Photoshop 4.0. Two frames showing the displacement of a particle over a known time span were combined using image analysis software developed by Data Translation. The displacement was measured in pixels, and those pixels were converted to a distance by comparison to a known distance in pixels. With this information, the average displacement velocity of the particle could be determined. To obtain the virtual velocity from the average displacement velocity, the only additional information needed was the average resting period of particles as they were transported downstream. The average displacement distance was divided by the sum of the average displacement time and the resting period to calculate the virtual velocity. Error encountered using the image analysis software and the repeatability of the results was less than 6-8%. The same technique has been used by Papanicolaou et al. (1999) to define displacement of particles.

The backbone of this methodology is based on the consideration that the lower limit for bedload motion is the incipient motion and the upper limit is saltation. Based on this consideration, the functional dependence of particle velocity on fluid, flow, and sediment bed parameters can be determined through the use of dimensional analysis (the Buckingham π theorem). This analysis yields six dimensionless π terms described in the following equation:

$$F\left(U_P^*\right) = F_1\left(\frac{w}{kU_*}, \frac{k_s}{d_i}, \frac{H}{d_i}, \frac{U_*^2}{gd_i\left(\rho_s/\rho - 1\right)}, \frac{U_* d_i}{\nu}, \left(\rho_s/\rho - 1\right)\right) \tag{4}$$

where $F(U^*_P)$ is a function of the dimensionless particle velocity, g is the gravitational acceleration, H is the average water depth, U_* is the friction velocity, κ is the von Karman constant, d_i is the diameter of the test material, k_s is the bed roughness, w is the fall velocity, ρ_s is the density of the test materials, ρ is the water density, and ν is the kinematic viscosity of water.

The first term on the right hand side of eq. 4 denotes the Rouse number, which is indicative of the mode of sediment motion. The second term in eq. 4 is the relative roughness term. The remaining terms are the relative submergence, the dimensionless bed shear stress τ_*, known as the Shields parameter, the particle Reynolds number Re_*, and the non-dimensional submerged weight of the test

material. Equation 4 can be further simplified if we account for the dependency of the dimensionless bed shear stress τ_* on the particle Reynolds number Re_*; combine the Rouse number with the dimensionless bed shear stress, and neglect the non-dimensional submerged weight of the test material, since it is already included in the shear stress term.
The simplified version of equation (4) is:

$$G\left(U_P^*\right) = F_2\left(\frac{w}{kU_*}, \frac{k_s}{d_i}, \frac{H}{d_i}, \frac{U_*^2}{gd_i\left(\rho_S/\rho - 1\right)}\right) \tag{5}$$

Equation (5) suggests that the displacement speed of particles is function of the variables shown on the right hand side of equation (5). In our experiments the roles of the Rouse number and relative submergence (defined in equation 1) have been negated, because the flow conditions correspond to bedload conditions and relative submergence is greater than 4. Hence, the U^*_P is function of k_s/d_i and $\frac{U_*^2}{gd_i\left(\rho_s/\rho - 1\right)}$.

Hence,
$$G\left(U_P^*\right) = F_2\left(, \frac{k_s}{d_i}, \frac{U_*^2}{gd_i\left(\rho_s/\rho - 1\right)}\right) \tag{6}$$

4. RESULTS

To validate the velocity profile obtained from the Swoffer current meter, depth-averaged velocity was calculated from the velocity profile and checked against the depth-averaged velocity calculated from the flow rate and depth (an error of less than 6% was recorded for all runs). It was found that the velocity profiles obtained with both instruments were well represented by the Log-Law

$$\frac{U}{U_*} = \frac{1}{\kappa}\ln\left(\frac{y}{k_s}\right) + B \tag{7}$$

where U is the average velocity at a distance, y, from the bed, U_* is the shear velocity, κ is the von Karmen constant taken to be 0.4, k_s is the equivalent sand grain bed roughness, and B is a constant of integration. The Log-Law velocity profiles were plotted linearly to determine U_* from the slope of the profile based on the Clauser method (1956) (Figure 5).

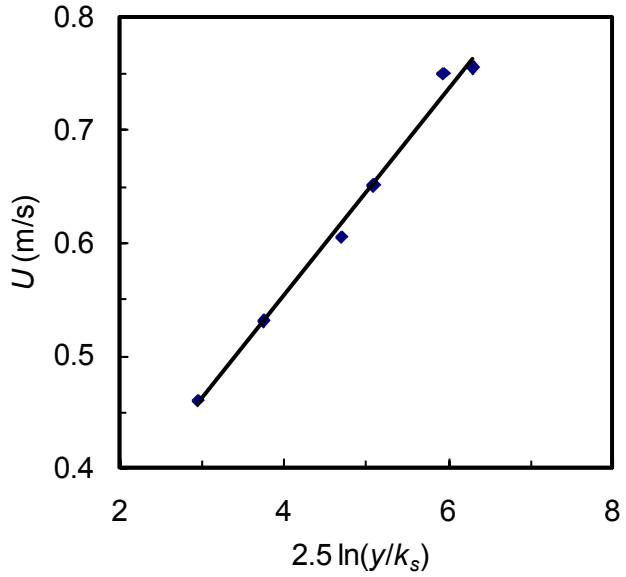

Figure 5. Velocity profile.

Because U_* relates to U through the log law (shown in eq. (7)), eq. (6) suggests that U_P can be expressed as function of U for a specified k_s / d_i ratio. Figure 6 shows that U is almost five times higher in magnitude than U_P: this is in agreement with the findings of Sun and Donohue (2000).

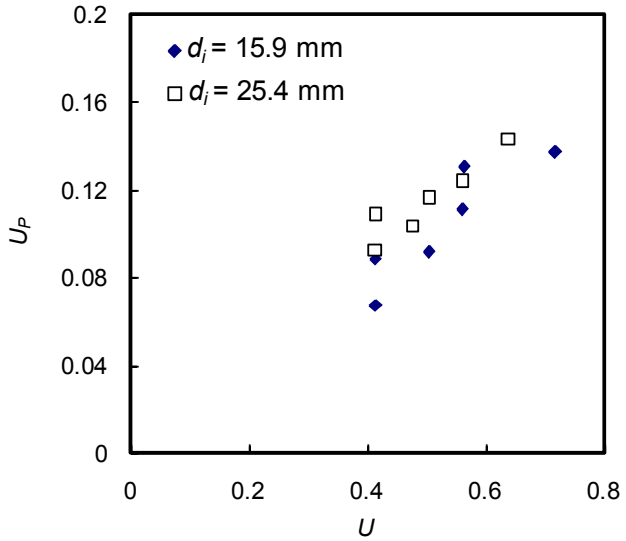

Figure 6. Particle velocity as function of the depth-averaged velocity.

The measured bedload rate was nondimensionalized as follows:

$$q_{s*} = \frac{q_s}{\sqrt{(\rho_s / \rho - 1) g d_i^3}} \tag{8}$$

and plotted against dimensionless bed shear stress τ_*

$$\tau_* = \frac{U_*^2}{(\rho_s / \rho - 1) g d_i} \tag{9}$$

where q_s is volumetric bedload rate per unit width For the three different particles sizes tested, it was found that $q_{s*} \propto \tau_*^{2.50}$ (Figure 7). This agrees with Paintal's (1971) data for bedload with relatively high shear stress values. The actual values of τ_* are lower than would be expected in the present study because of the well-packed uniform bed on which the test particles were placed.

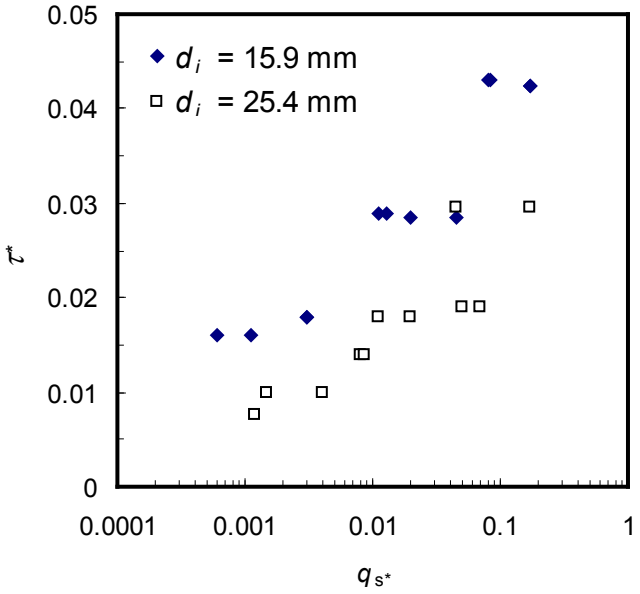

Figure 7. Bed shear stress versus bedload discharge.

Video tape was analyzed to determine the number of times a particle actually hit the cylinder per run, actual hits, and how many times the flow around the cylinder influenced the particle to go around the cylinder instead of hitting it. The term theoretical hits is used to describe the sum of actual hits and the number that were influenced by the flow around the cylinder. Measured bedload was compared to the predicted bedload from the recorded impacts as well as the theoretical impacts to assure that a representative portion of the bedload was passing through the occupied cylinder area (Figure 8). The measured and theoretical bedload rates compare well to each other, showing that the number of particles on path to hit the cylinder area can be applied to the rest of the bed.

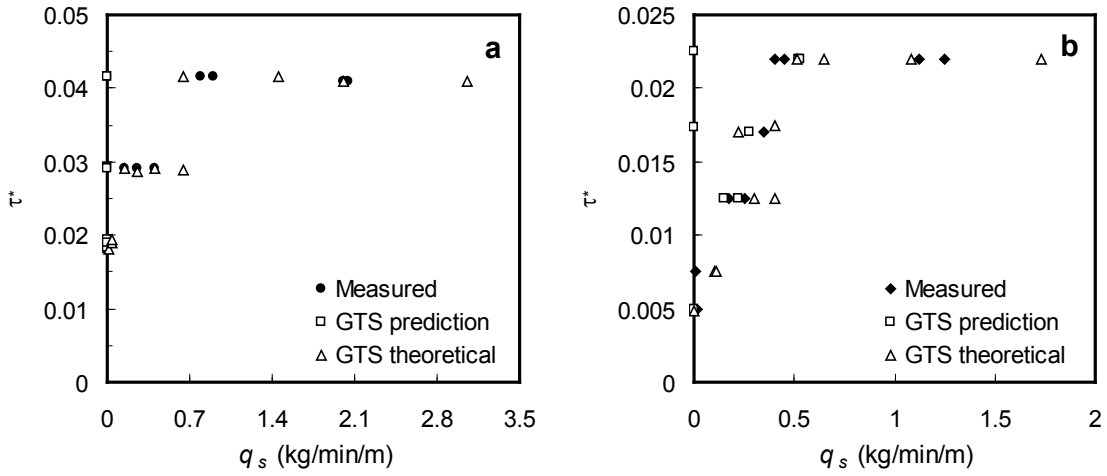

Figure 8. Comparison of theoretical and measured bed load: a) di = 15.9 mm; b) di = 25.4 mm.

The percentage of theoretical and actual impacts, or pings, were thereafter compared to the percentage of impacts recorded by the GTS (Figure 9). It was found that as the velocity of the fluid increased, the ability of the GTS to detect particles heading towards it decreased. Its ability to detect the particles also decreased with particle size. Figure 10 shows that with a decrease in particle size, theoretical hits increased while recorded hits decreased. It is worth noting that for the smallest size tested, d_i = 15.9 mm (5/8 in), the GTS did not detect any particles.

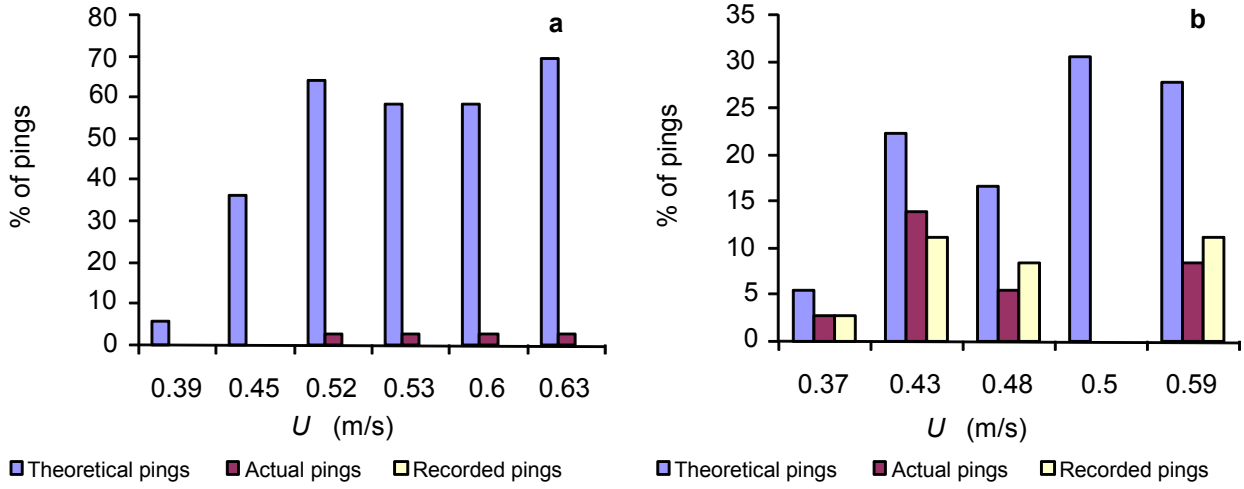

Figure 9. Comparison between theoretical, actual, and recorded pings: a) d_i = 15.9 mm; b) d_i = 25.4 mm.

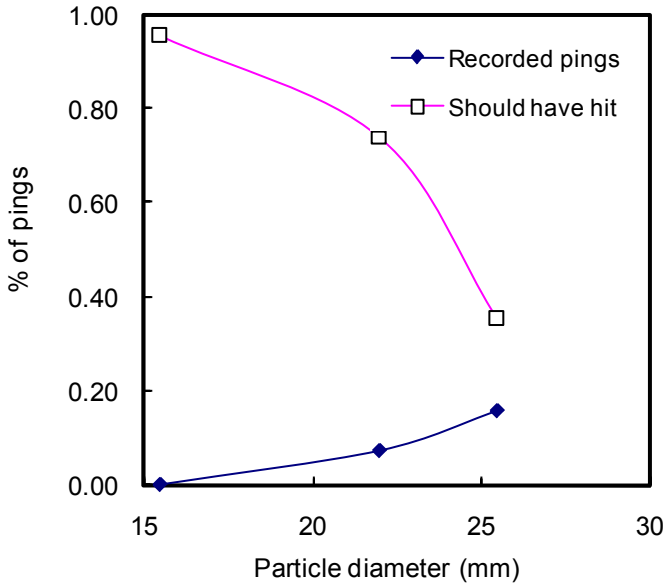

Figure 10. Comparison between theoretical and recorded pings.

This trend in figure 10 can partly be explained by changes in flow due to the presence of the cylinder. As the flow approaches the cylinder with an angle of attack $\alpha = 0^o$, as defined in figure 11 where z is in the vertical direction, U(y) diminishes considerably and close to the bed a flow reversal is established (Graf and Yulistiyanto, 1998) (figure11). Flow going around the cylinder undergoes an acceleration and as $\alpha \rightarrow 45^o$, V(y), the velocity in the transverse direction, increases and reaches values of the same order of magnitude as U(y) (Graf and Yulistiyanto, 1998). In front of the cylinder the separation point is influenced by the negative W(y) component, where W(y) is the velocity in the vertical plane. Through experiments for air flow around cylinders, Belik (1973), found the following relation (eq. 4) to be true for $2.2\times10^5 > Re_\delta > 3.6\times10^4$.

$$\frac{a}{D} = 0.57(2\times10^{-5}\times Re_\delta)^{0.19} \qquad (10)$$

where, a is the distance along the bed from the cylinder to the point of separation, D is the diameter of the cylinder, and $Re_\delta = U_e\delta/\nu$. For open channel flow, δ can be taken as the depth of flow h. Graf and Yulistiyanto (1998) applied equation (10) to a combination of air flow and free surface flow data in the range of $11.5\times10^5 > Re_h > 1.6\times10^3$ and found it to be valid. Hence, as Re_h increases, so does the distance of the separation point form the cylinder at a position of $\alpha = 0^o$. The values of Re_h for the present study fell within the range examined by Graf and Yulistiyanto (1998).

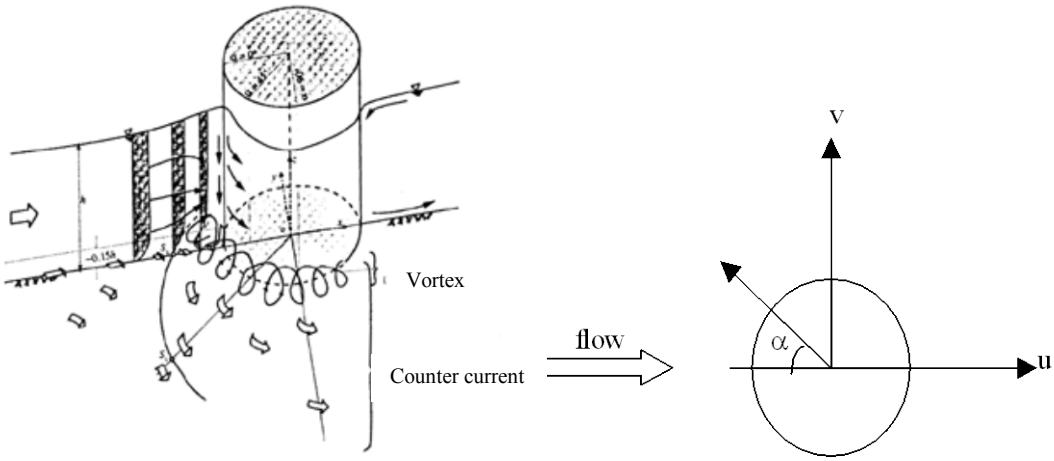

Figure 11. Flow around a cylinder (after Graf and Yulistiyanto, 1998).

This flow reversal in front of the cylinder can have an effect on the particles moving as bedload. It was observed during test with the smallest size, 15.9 mm (5/8 in), that before they hit the cylinder, particles come to rest and cluster (fig. 12). Formation of these clusters would greatly reduce the GTS's ability to accurately measure bedload.

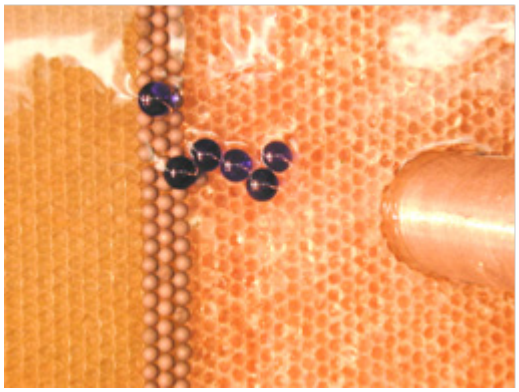

Figure 12. Clustering of particles.

5. CONCLUSIONS

The development of the GTS is a necessary step to better understand sediment transport in gravel bed channels, especially for low flow conditions. Its ability to make unattended local measurements, record data over long periods of time, capture the larger size fractions, and the ease of movement are all advantages the GTS has over the other current techniques. Testing on the prototype model showed that the ability of the GTS to make accurate measurements increases as particle size increases. The presence of the cylinder in the flow can have a large effect on the smaller sized particles and cause them to follow the streamlines around the cylinder rather than impacting it. Further testing needs to be conducted to find particle velocity under varying flow conditions and relate its momentum to the detection rate of the GTS. The prototype GTS is only in its first stages. Further development of the GTS piezoelectric vibration sensor will allow for an improved correlation between the momentum

of a particle and the acoustic output signal. This will allow the GTS to record a particles momentum to account for non-uniformity in the bed material. In addition, a modification of the cylindrical shape of the GTS to a rhomboid shape in order to minimize flow reversal will probably improve the effectiveness of the instrument (figure 13).

Figure 13. Proposed modification of the GTS shape.

Finally, the developed particle velocity equations have great potential for bedload applications and the instantaneous particle velocity equation can be used to calibrate the GTS. Also, the virtual velocity relation can be used to develop a bedload transport equation. The study showed that the virtual velocity is about 5 times less in magnitude than the flow velocity. The size of the entrained particle versus the size of the bed is a key factor in the resting period that affects the overall movement of a particle. Future work on the virtual velocity and the excess shear correction is warranted.

ACKNOWLEDGEMENTS

The authors would like to acknowledge the financial support provided by the Washington Technology Center for the completion of this research. The project was partly supported by Dr. John Downing (D&A instruments) with matching funds. The authors would like to thank Kyle Strom for helping with some of the preliminary experiments, and the two reviewers Dr. Thomas Buffin-Bélanger and Dr. Alain Recking for their comments which have helped to immensely improve the quality of this manuscript.

REFERENCES

Bunte, K. (1992). "Particle Number Grain-size Composition of Bedload in a Mountain Stream.", In: Billi, P., Hey, R.D., Thorne, C.R., and Tacconi, P. (ed.), Dynamics of Gravel-bed Rivers, John Wiley and Sons, Chichester, UK.

Church, M.A., McLean, D.G., and Wolcott, J.F. (1987). "River Bed Gravels: Sampling and Analysis", In: Thorne, C.R., Bathurst, J.C, and Hey, R.D. (ed.), Sediment Transport in Gravel-bed Rivers, John Wiley and Sons, Chichester, UK.

Clauser, F. (1956). "The Turbulent Boundary Layer", Advances in Applied Mechanics, Vol. 4, pp. 1-51.

Downing, J. (1999). GTS Instruction Manual, D & A Instrument Company, Port Townsend, WA.

Graf, W.H., and Yulistiyanto, B., (1998). "Experiments on flow around a cylinder; the velocity and vorticity fields", Journal of Hydraulic Research, IAHR, 36(4), pp. 637-653

Leaf, C.F. (1970). "Sediment Yields from Central Colorado Snow Zone", Journal of the Hydraulic Division, ASCE, Vol. 96, No. HY1, pp. 87-93.

Lee, H-Y., Chen, Y-H., You, J-Y., and Lin, Y-T. (2000). "Investigations of Continuous Bed Load Saltating Process", Journal of Hydraulic Engineering, ASCE, Vol. 126, No. 9, pp. 691-700.

Paintal, A.S. (1971). "Concept of Critical Shear Stress in Loose Boundary Open Channels", Journal of Hydraulic Research, Vol. 9, No.1, pp. 91-113.

Papanicolaou, A., Diplas, P., Balakrishnan, M., and Dancey, C.L. (1999). **"**Computer Vision Techniques for Sediment Transport", Journal of Computing in Civil Engineering, ASCE, Vol. 13, No. 2, pp. 71-79.

Papanicolaou, A., Diplas, P., Evaggelopoulos, N., and Fotopoulos, S**.** (2002). "A Stochastic Incipient Motion Criterion for Spheres under Various Bed Packing Conditions", Journal of Hydraulic Engineering, ASCE, Vol. 128, No. 4, pp. 369-380.

Ryan, S.E. and Troendle, C.A. (1997). "Measuring Bedload in a Coarse-Grained Mountain Channels: Procedures, Problems, and Recommendations", Proceedings of the American Water Resources Association Annual Summer Conference, pp. 949-958.

Sekine, M., and Kikkawa, H. (1992). "Mechanics of Saltating Grains, II", Journal of Hydraulic Engineering, ASCE, Vol. 118, pp. 536-558.

Sun, Z. and Donahue, J. (2000). "Statistically Derived Bedload Formula for any Fraction of Nonuniform Sediment," *Journal of Hydraulic Engineering*, vol. 126, no. 2, 105-111.

Troendle, C.A., Nankervis, J.M., and Ryan, S.E. (1996). "Sediment Transport from Small, Steep-Gradient Watersheds in Colorado and Wyoming", In: Sedimentation Technologies for Management of Natural Resources in the 21st Century, Sixth Federal Interagency Sedimentation Conference, pp. IX-39-IX45.

USGS Office of Surface Water. (1990). "Programs and Plans - Policy and Guidelines for the Collection and Publication of Bedload Data", USGS Office of Surface Water Technical Memorandum No. 90.08, Reston, VA.